Change in the Micellar Aggregation Number or in the Size Distribution? A Dynamic Fluorescence Quenching Study of Aqueous Cetyltrimethylammonium Chloride

Steven Reekmans,† Delia Bernik,‡ Marcello Gehlen,§ Jan van Stam,⊥ Mark Van der Auweraer,† and Frans C. De Schryver*,†

Department of Chemistry, Katholieke Universiteit Leuven, Celestijnenlaan 200F, B-3001 Heverlee, Belgium, Instituto de Investigaciones Fisicoquímicas Teóricas y Aplicadas, La Plata, Argentina, Instituto de Física e Química de São Paulo, Brazil, and Department of Physical Chemistry, University of Uppsala, P.O. Box 532, S-751 21 Uppsala, Sweden

Received April 15, 1993. In Final Form: June 15, 1993

Aqueous solutions of cetyltrimethylammonium chloride were studied by means of dynamic fluorescence quenching measurements to get information on the micellar aggregation number and size polydispersity as a function of surfactant concentration. The global analysis of multiple decay curves provided estimates with improved accuracy and precision and indicated a reduced polydispersity upon increasing surfactant concentration. As the quenching rate slows with increasing surfactant concentration it is concluded that there is a micellar growth, but that this growth preferably increases the aggregation number for the smaller aggregates in the initially polydisperse solutions.

1. Introduction

Micellar solutions are to be considered as microheterogeneous with micellar entities of dimensions intermediate between those of single molecules and macroscopic objects. Micelles and micellar dynamics are of interest in various fields (e.g., paints, pharmaceutical drugs, and enhanced oil recovery), and have been intensively studied the few last decades, both theoretically and experimentally.[1-4] Various techniques have been applied in the study of micellar characteristics; one may distinguish between experimental methods that make use of intrinsic properties of the system and methods that make use of solubilized probe molecules. Within the first category one find methods such as, e.g., light-scattering and NMR, and in the latter, among others, methods based on the fluorescence of a probe molecule.

Differences in experimental results published over the years may be due to the advances of the various techniques and the improved analysis of experimental and synthetic data, as well as the fact that different methods measure different properties of the system. One must therefore keep in mind what one really compares when results obtained with different methods are discussed. This is certainly to be considered for micellar systems, where fluorescence quenching techniques and light-scattering techniques are among the most popular. In this paper, the discussions are limited to results obtained with dynamic fluorescence quenching, which is a well-described method for measurement of relevant parameters in microheterogeneous systems.[5-8]

Many data on micellar size and shape of various surfactant systems, both without additives and in the presence of, e.g., salt,[9-11] alcohols,[12-15] or polymers,[16-21] have been published. Variations in the choice of method (static versus dynamic fluorescence quenching) or in the experimental composition, e.g., choice of probe–quencher pair, may influence the results obtained for a given surfactant system. The effect of the probe–quencher pair chosen is of fundamental significance, as, e.g., excimer formation versus probe–quencher encounter complexes and mobile versus immobile species influence the overall

* To whom correspondence should be addressed.
† Katholieke Universiteit Leuven.
‡ Instituto de Investigaciones Fisicoquímicas Teóricas y Aplicadas.
§ Universidade de São Paulo.
⊥ University of Uppsala.

(1) a. Wennerström, H.; Lindman, B. *Phys. Rep.* **1979**, *52*, 1. b. Lindman, B.; Wennerström, H. *Top. Curr. Chem.* **1980**, *87*, 1.
(2) Tanford, C. *The Hydrophobic Effect*; John Wiley & Sons: New York, 1980.
(3) Israelachvili, J. N.; Mitchell, D. J.; Ninham, B. W. *J. Chem. Soc., Faraday Trans. 2* **1976**, *72*, 1525.
(4) a. Nagarajan, R.; Ruckenstein, E. *J. Colloid Interface Sci.* **1979**, *71*, 580. b. Nagarajan, R.; Ruckenstein, E. *J. Colloid Interface Sci.* **1983**, *91*, 500.
(5) a. Almgren, M. In *Kinetic and Catalysis in Microheterogeneous Systems*; Grätzel, M., Kalyanasundaram, K., Eds.; Marcel Dekker: New York, 1991; p 63. b. Almgren, M. *Adv. Colloid Interface Sci.* **1992**, *41*, 9.
(6) Grieser, F.; Drummond, C. *J. Phys. Chem.* **1988**, *92*, 5580.
(7) a. Van der Auweraer, M.; De Schryver, F. C. In *Inverse Micelles, Studies in Physical and Theoretical Chemistry*; Pileni, M. P., Ed.; Elsevier: Amsterdam, 1990; p 70. b. Gehlen, M.; De Schryver, F. C. *Chem. Rev.* **1993**, *93*, 199.
(8) a. Zana, R. In *Surfactant Solutions. New Methods of Investigation*; Zana, R., Ed.; Marcel Dekker: New York, Basel, 1987; p 241. b. Zana, R.; Lang, J. *Colloids Surf.* **1990**, *48*, 153.
(9) a. Croonen, Y.; Geladé, E.; Van den Zegel, M.; Van der Auweraer, M.; De Schryver, F. C. *J. Phys. Chem.* **1983**, *87*, 1426. b. Reekmans, S.; De Schryver, F. C. In *Frontiers in Supramolecular Organic Chemistry and Photchemistry*; Schneider, H. J., Durr, H., Eds.; VCH: New York, 1991; p 287.
(10) Söderman, O.; Jonströmmer, M.; van Stam, J. *J. Chem. Soc., Faraday Trans.* **1993**, *89*, 1759.
(11) Binana-Limbelé, W.; van Os, N. M.; Rupert, L. A. M.; Zana, R. *J. Colloid Interface Sci.* **1991**, *144*, 458.
(12) Reekmans, S.; Luo, H.; Van der Auweraer, M.; De Schryver, F. C. *Langmuir* **1990**, *6*, 628.
(13) Almgren, M.; Swarup, S. *J. Colloid Interface Sci.* **1983**, *91*, 256.
(14) Luo, H.; Boens, N.; Van der Auweraer, M.; De Schryver, F. C.; Malliaris, A. *J. Phys. Chem.* **1989**, *93*, 3244.
(15) Malliaris, A.; Lang, J.; Sturm, J.; Zana, R. *J. Phys. Chem.* **1987**, *91*, 1475.
(16) van Stam, J.; Brown, W.; Fundin, J.; Almgren, M.; Lindblad, C. In *Colloid-Polymer Interactions*; Dubin, P. L., Tong, P., Eds.; ACS Symposium Series; American Chemical Society: Washington, DC, in press.
(17) a. Cabane, B.; Duplessix, R. *J. Phys.* **1982**, *43*, 1529. b. Cabane, B.; Duplessix, R. *Colloids Surf.* **1985**, *13*, 19. c. Cabane, B.; Duplessix, R. *J. Phys.* **1987**, *48*, 651.
(18) Goddard, E. D. *Colloids Surf.* **1986**, *19*, 255.
(19) Reekmans, S.; Gehlen, M.; Van der Auweraer, M.; Boens, N.; De Schryver, F. C. *Macromolecules* **1993**, *26*, 687.
(20) Thalberg, K.; van Stam, J.; Lindblad, C.; Almgren, M.; Lindman, B. *J. Phys. Chem.* **1991**, *95*, 8975.
(21) Lindman, B.; Thalberg, K. In *Polymer-Surfactant Interactions*; Goddard, E. D., Ananthapadmanabhan, K. P., Eds.; CRC Press: Boca Raton, FL, in press.

0743-7463/93/2409-2289$04.00/0

quenching and diffusion processes, and, thereby, the choice of model to obtain, e.g., the micellar aggregation number. This choice or the interpretation of the obtained results from model fittings is often not obvious, and may lead to ambiguous conclusions.

For many micellar systems, one important question is whether the micellar aggregates grow upon increasing surfactant concentration or changes in the obtained information on the system are due to aggregate size polydispersity.[22-24] One must be careful in generalizing tendencies such as micellar growth for different surfactant systems, as the length of the hydrophobic tail, the size of the polar head group, and counterions all play a critical role in the definition of micellar shape and size. Furthermore, ionic detergent molecules, although characterized by an identical alkyl chain and headgroup, may exert a different behavior in their interaction with additives, such as inorganic salts[9] or nonionic polymer,[18] if counterions of different electronegativity are shielding the headgroup charges.[25,26] In the literature one finds examples, such as the surfactant cetyltrimethylammonium ion with bromide (CTAB) or chloride (CTAC) as counterion, whose shape transitions as a function of detergent concentration and added salt concentration have been extensively studied.[20,27-32] Parameters such as the critical micellization concentration (cmc) and the aggregation number are dependent on the counterion. The surfactant is known to form huge, wormlike micelles in the presence of sodium salicylate[33] or perchlorate.[24b,c] In the absence of additives it is thought that the micelles formed go through regions with aggregate growth, an increase of the number of micelles without significant changes in the aggregate size, and shape transitions upon addition of more surfactant.[34]

In a recent publication on the probe (1-pyrenesulfonate) migration process in CTAC micellar systems no micellar growth was detected,[30c] whereas previous results obtained by single curve analysis of dynamic fluorescence quenching data pointed out an increase of the aggregation number within this concentration range.[30a]

In this paper, we have chosen to illustrate the influence of surfactant concentration and choice of some experimental parameters on the micellar aggregation number and size polydispersity for cetyltrimethylammonium chloride (CTAC) as determined by dynamic fluorescence quenching (DFQ). The fluorescence probe used was 1-methylpyrene (1-MePy) and the quencher hexadecylpyridinium chloride (CPyrC). Careful, global analysis of data clearly indicates that the aggregates do not grow in size (or equally, aggregation number), but change from a rather polydisperse aggregation behavior close to cmc to a more monodisperse behavior at higher surfactant concentrations.

2. Experimental Section and Theory

2.1. Chemicals. *1-Methylpyrene* (1-MePy) was synthesized and purified as described by Roelants et al.[35] 1-MePy in deoxygenated methanol solution showed a monoexponential fluorescence decay with a decay time of 190 ± 2 ns at room temperature.

Hexadecyltrimethylammonium chloride (CTAC; Kodak) contained fluorescent impurities and was purified by Soxhlet extraction with diethyl ether followed by recrystallization from a 10/1 (v/v) acetone–methanol mixture. 1-MePy in a deoxygenated CTAC solution showed a monoexponential decay (190 ± 4 ns) at room temperature.

Hexadecylpyridinium chloride (CPyrC; Henkel) did not show any fluorecent impurities and was used as received.

2.2. Experimental Conditions. Fluorescent decay curves were obtained with the same equipment and setup as described previously.[36] The excitation wavelength was 325 nm, and the emission was monitored at 380 nm. All fluorescence decay curves were observed at the magic angle (54.7°), contained 10^4 peak counts, and were collected in 512 channels of the multichannel analyzer. Time increments of ~0.8 ns/channel and ~1.7 ns/channel were used, with anthracene (lifetime 5.6 ns) and 1-cyanopyrene (lifetime 21.6 ns) as references, respectively, to check the importance of the width of the time window for the observed fluorescence decay. At every CTAC concentration (7, 10, 20, and 40 mM), eight CPyrC concentrations were chosen such that the average numbers of quenchers per micelle varied from ~0.4 to ~2.3, whereas samples without added quencher provided monoexponential, unquenched decays.

The probe concentration was always kept low enough to prevent excimer formation.

All measurements were, if not mentioned otherwise, performed at room temperature (~20 °C). All solutions were prepared with water of Milli-Q quality and deoxygenated by repeated freeze–pump–thaw cycles.

2.3. Dynamic Fluorescence Quenching. In a dynamic fluorescence quenching (DFQ) experiment the fluorescence decay of an excited probe is analyzed by appropriate kinetic models to recover parameters giving information about structural and/or photophysical changes in the system.

The basic relation is the well-known Infelta–Tachiya model[37,38]

$$Ft = A_1 \exp[-A_2 t - A_3\{1 - \exp(-A_4 t)\}] \quad (1)$$

developed under the assumptions that the micellar aggregates are of equal size, the fluorescence probe is stationary in its host micelle during the time for the photophysical processes, the probe and the quencher molecules are distributed in a Poissonian way among the micelles, and the quencher molecules do not interact with each other.

In this model, the parameters A_1–A_4 were given the following expressions:[37]

(22) Almgren, M.; Löfroth, J.-E. *J. Chem. Phys.* **1982**, *76*, 2734.
(23) a. Warr, G.; Grieser, F. *J. Chem. Soc., Faraday Trans. 1* **1986**, *82*, 1813. b. Warr, G.; Grieser, F.; Evans, D. F. *J. Chem. Soc., Faraday Trans. 1* **1986**, *82*, 1829.
(24) a. Almgren, M.; Alsins, J. *Prog. Colloid Polym. Sci.* **1987**, *74*, 55. b. Almgren, M.; Alsins, J.; van Stam, J.; Mukhtar, E. *Prog. Colloid Polym. Sci.* **1988**, *76*, 68. c. Almgren, M.; Alsins, J.; Mukhtar, E.; van Stam, J. *J. Phys. Chem.* **1988**, *92*, 4479. d. Almgren, M.; Alsins, J.; Mukhtar, E.; van Stam, J. In *Reactions in Compartmentalized Liquids*; Knoche, W., Schomäcker, R., Eds.; Springer Verlag: Berlin, Heidelberg, 1989; p 61.
(25) Almgren, M.; Löfroth, J.-E.; Rydholm, R. *Chem. Phys. Lett.* **1979**, *63*, 265.
(26) Saito, S.; Kitamura, K. *J. Colloid Interface Sci.* **1971**, *35*, 346.
(27) Lianos, P.; Viriot, M. L.; Zana, R. *J. Phys. Chem.* **1984**, *88*, 1098.
(28) Malliaris, A.; Lang, J.; Zana, R. *J. Chem. Soc., Faraday Trans. 1* **1986**, *82*, 109.
(29) Witte, F. M.; Engberts, J. *J. Org. Chem.* **1987**, *52*, 4767.
(30) a. Roelants, E.; De Schryver, F. C. *Langmuir* **1987**, *3*, 209. b. Malliaris, A.; Boens, N.; Luo, H.; Van der Auweraer, M.; Reekmans, S.; De Schryver, F. C. *Chem. Phys. Lett.* **1989**, *155*, 587. c. Gehlen, M.; Boens, N.; De Schryver, F. C.; Van der Auweraer, M.; Reekmans, S. *J. Phys. Chem.* **1992**, *96*, 5592.
(31) Brackman, J.; Engberts, J. *Langmuir* **1991**, *7*, 2097.
(32) a. Sjöberg, M.; Henriksson, U.; Wärnheim, T. *Langmuir* **1990**, *6*, 1205. b. Sjöberg, M.; Jansson, M.; Henriksson, U. *Langmuir* **1992**, *8*, 409.
(33) a. Shikata, T.; Hirata, H.; Kotaka, T. *Langmuir* **1988**, *4*, 354. b. Hirata, H.; Sakaiguchi, Y.; Akai, J. *J. Colloid Interface Sci.* **1989**, *127*, 589. c. Ruckenstein, E.; Brunn, P. O.; Holweg, J. *Langmuir* **1988**, *4*, 350.
(34) a. Blackmore, E. S.; Tiddy, G. J. T. *J. Chem. Soc., Faraday Trans. 2* **1988**, *84*, 1115. b. Henriksson, U.; Blackmore, E. S.; Tiddy, G. J. T.; Söderman, O. *J. Phys. Chem.* **1992**, *96*, 3894.
(35) Roelants, E.; Geladé, E.; Van der Auweraer, M.; De Schryver, F. C. *J. Colloid Interface Sci.* **1983**, *96*, 288.
(36) a. Boens, N.; Van den Zegel, M.; De Schryver, F. C.; Desie, G. In *From Photophysics to Photobiology*; Favre, A., Tyrell, R., Cadet, J., Eds.; Elsevier: Amsterdam, 1987; p 93. b. Khalil, M. M. H.; Boens, N.; Van der Auweraer, M.; Ameloot, M.; Andriessen, R.; Hofkens, J.; De Schryver, F. C. *J. Phys. Chem.* **1991**, *95*, 9375.
(37) a. Infelta, P. P.; Grätzel, M.; Thomas, J. K. *J. Phys. Chem.* **1974**, *78*, 190. b. Infelta, P. P.; Grätzel, M. *J. Chem. Phys.* **1983**, *78*, 5280.
(38) a. Tachiya, M. *Chem. Phys. Lett.* **1975**, *33*, 289. b. Tachiya, M. *J. Chem. Phys.* **1982**, *76*, 340. c. Tachiya, M. *J. Chem. Phys.* **1983**, *78*, 5282. d. Sano, H.; Tachiya, M. *J. Chem. Phys.* **1981**, *75*, 2870.

$$A_1 = F_0 \tag{2a}$$

$$A_2 = k_0 + k_q k_+ Q_f/(k_q + k_-) \tag{2b}$$

$$A_3 = K_I k_q^2 Q_f/(k_q + k_-)^2 \tag{2c}$$

$$A_4 = k_q + k_- \tag{2d}$$

where F_0 is the intensity at time $t = 0$, k_0 is the fluorescence decay rate constant in the absence of added quencher, k_q is the first-order rate constant for quenching by one quencher in a micelle, k_+ is the second-order rate constant for the entry of quenchers from the bulk into a micelle, k_- is the first-order rate constant for one quencher to exit from a micelle to the bulk, Q_f is the concentration of free quenchers in the bulk ($Q_f = Q_t - Q_m$, indices t and m denoting total and micelle-bound, respectively), and K_I, the distribution constant for quenchers between micelles and the bulk, is equal to k_+/k_-.

In the case of an immobile quencher, i.e., $k_q \gg k_-$ and $k_0 \gg k_+Q_f$, eq 1 reduces to a much simpler form:

$$F_t = F_0 \exp[-k_0 t - \langle n\rangle\{1 - \exp(-k_q t)\}] \tag{3}$$

where $\langle n\rangle$ is the average occupation number of quenchers in a micelle, $\langle n\rangle = Q_m/[\text{micelle}]$. From $\langle n\rangle$ the aggregation number, $\langle a\rangle$, is easily obtained:

$$\langle a\rangle = \langle n\rangle S_m/Q_m \tag{4}$$

where S_m is the amount of micellized surfactant. In this paper we set $S_m = S_t - \text{cmc}$, with cmc = 1.3 mM.[39]

For the case of migrating probes and quenchers, generalized versions of the Infelta–Tachiya model have been developed.[40,41]

In a monodisperse system, one can make use of the relation between $\langle n\rangle$ and Q_m, as a plot of the former versus the latter should yield a straight line through the origin with a slope equal to 1/[micelle]. From this slope, k_m, the aggregation number for the monodisperse micelles, $\langle a\rangle_m$, can be calculated by

$$\langle a\rangle_m = k_m S_m \tag{5}$$

If the system is not monodisperse, but shows a broader size distribution, it is shown[22] that the fluorescence decay still is well described by an expression like eq 3. Within each subset of the system, differing in aggregation number, the probe and quencher molecules will be distributed in a Poissonian way. The distribution of molecules between the different subsets will, however, be weighted by the relative volume of each subset; i.e., for low quencher concentrations, the quencher molecules will be preferably solubilized in the larger aggregates. The obtained aggregation numbers will in such a case be dependent on the quencher concentration, and should be treated as a quencher-averaged aggregation number, $\langle a\rangle_q$.[22,23] From $\langle a\rangle_q$ it is possible to calculate a weight-averaged aggregation number, $\langle a\rangle_w$, which is independent of the quencher concentration, by

$$\langle a\rangle_q = \langle a\rangle_w - {}^1/_2\sigma^2\eta + {}^1/_6\kappa\eta^2 - \ldots \tag{6}$$

where σ^2 is the variance and κ the third cumulant, giving the skewness, of the size distribution. η is given by

$$\eta = Q_m/S_m \tag{7}$$

The quota $\sigma/\langle a\rangle_w$ can be used as a "polydispersity index", showing trends in the size distribution.

The eight different fluorescence decays at each surfactant concentration were analyzed simultaneously, and use was made of the relations between different curves by linking appropriate decay parameters in the global mapping table.[37b] The models used were computed by a global[42,43] iterative reweighted reconvolution program based on the Marquardt algorithm for nonlinear least squares.[44] All computations were performed on an IBM 6000/RISC computer with the programs developed by Boens et al.[45]

Table I. Rate Constants, Decay Times, and Associated Parameters for the Fluorescence Quenching of 1-MePy (10^{-5} M) by CPyrC in the Four CTAC Micellar Systems, Recovered by Simultaneous Analysis of Eight Decay Curves, Where Equation 3 Was Fitted to the Data[a]

[CTAC], mM	[Q], mM	τ_0, ns	$\langle n\rangle$	k_q, 10^7 s^{-1}	$\lvert Z(\chi_\nu^2)\rvert$ individual	$\lvert Z(\chi_\nu^2)\rvert$ global
7	0.025	185 ± 1	0.382 ± 0.004	1.40 ± 0.01	1.127	2.935
	0.041		0.530 ± 0.004		2.049	
	0.058		0.744 ± 0.005		0.982	
	0.082		1.044 ± 0.005		0.041	
	0.120		1.430 ± 0.005		0.658	
	0.140		1.751 ± 0.005		1.127	
	0.170		1.954 ± 0.006		1.474	
	0.190		2.268 ± 0.006		2.857	
10	0.035	188 ± 1	0.357 ± 0.005	1.33 ± 0.01	1.299	1.617
	0.059		0.545 ± 0.005		0.165	
	0.094		0.846 ± 0.005		0.172	
	0.150		1.278 ± 0.005		0.296	
	0.180		1.521 ± 0.005		0.844	
	0.210		1.762 ± 0.005		2.146	
	0.240		1.982 ± 0.006		0.870	
	0.270		2.276 ± 0.006		0.732	
20	0.071	187 ± 1	0.329 ± 0.005	1.23 ± 0.01	2.119	3.033
	0.120		0.538 ± 0.005		1.133	
	0.160		0.671 ± 0.007		1.736	
	0.240		1.057 ± 0.006		0.675	
	0.330		1.484 ± 0.006		2.244	
	0.400		1.715 ± 0.006		1.337	
	0.470		2.015 ± 0.006		2.102	
	0.540		2.314 ± 0.007		0.589	
40	0.240	193 ± 1	0.576 ± 0.008	1.04 ± 0.01	3.555	2.707
	0.480		1.162 ± 0.007		2.328	
	0.660		1.598 ± 0.008		0.312	
	0.800		1.909 ± 0.007		0.338	
	0.940		2.247 ± 0.007		0.449	
	1.080		2.572 ± 0.008		1.447	

[a] The time increment was ~0.8 ns/channel, and the reference was anthracene (τ_r = 5.6 ns).

3. Results and Discussion

3.1. Use of Global Analysis of Multiple Fluorescence Decay Curves To Determine Model Parameters. From the observed fluorescence decays, shown for the room-temperature measurements at the two time increments in Figure 1, one can draw conclusions about the mobility of the probe and quencher. First, the emission from samples without added quencher yields decays without curvature in the logarithmic representation, showing neither excimer formation nor a significant distribution of the probe between the micelles and the aqueous bulk phase. Second, as, from both visual inspection of the decay curves and from fittings, the decay curves for the same surfactant concentration at all quencher concentrations show parallel monoexponential tails at long times, independent of the time increment, it can be concluded that neither the probe nor the quencher migrates during the time window studied. This allows us to make use of the simplified Infelta–Tachiya model, eq 3. The results, judged by the statistical fitting parameter $Z(\chi_\nu^2)$,[45] from fittings of eq 3 to data obtained at the short time increment are summarized in Table I. In these fittings

(39) Almgren, M.; Hansson, P.; Mukhtar, E.; van Stam, J. *Langmuir* **1992**, *8*, 2405.
(40) Almgren, M.; Löfroth, J.-E.; van Stam, J. *J. Phys. Chem.* **1986**, *90*, 4431.
(41) Gehlen, M.; Van der Auweraer, M.; De Schryver, F. C. *Langmuir* **1992**, *8*, 64.
(42) Knutson, J. R.; Beechem, J. M.; Brand, L. *Chem. Phys. Lett.* **1983**, *102*, 501.
(43) a. Löfroth, J.-E. *Eur. Biophys. J.* **1985**, *13*, 45. b. Löfroth, J.-E. *J. Phys. Chem.* **1986**, *90*, 1160.
(44) a. Ameloot, M.; Hendrickx, H. *J. Chem. Phys.* **1982**, *76*, 4419. b. Marquardt, D. W. *J. Soc. Ind. Appl. Math.* **1963**, *11*, 431. c. Van den Zegel, M.; Boens, N.; Daems, D.; De Schryver, F. C. *Chem. Phys.* **1986**, *101*, 311.
(45) a. Boens, N.; Malliaris, A.; Van den Auweraer, M.; Luo, H.; De Schryver, F. C. *Chem. Phys.* **1988**, *121*, 199. b. Reekmans, S.; Boens, N.; Van der Auweraer, M.; Luo, H.; De Schryver, F. C. *Langmuir* **1989**, *5*, 948.

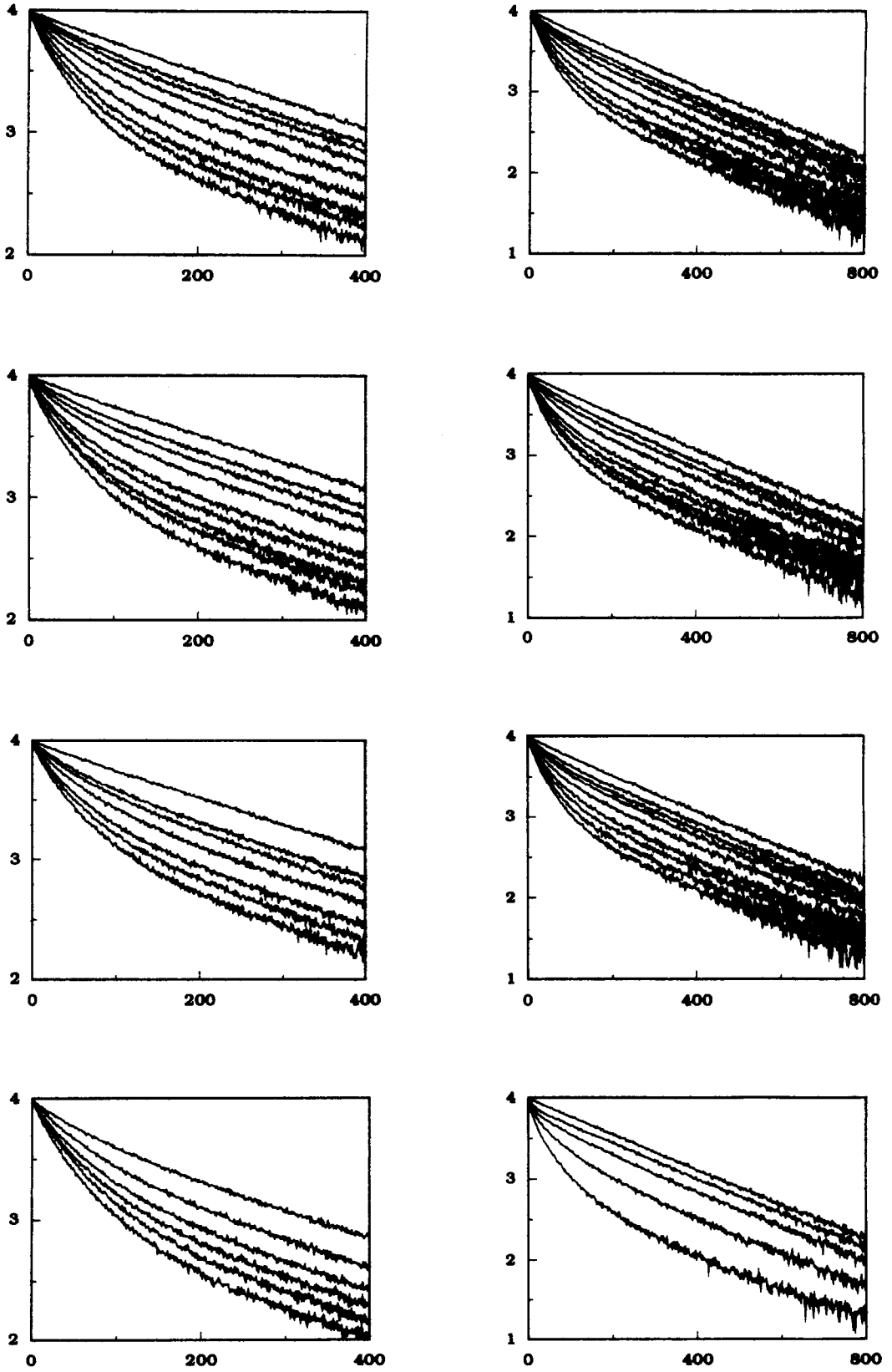

Figure 1. Fluorescence decay curves at the different CTAC concentrations (7, 10, 20, and 40 mM CTAC from top to bottom) and at the two different time increments used (left column, ~0.8 ns/channel; right column, ~1.7 ns/channel). The x axis gives the time (ns) and the y axis the logarithm of the (normalized) amount of counts per channel. For 7 and 10 mM CTAC at both time increments and 20 mM CTAC observed at 1.7 ns/channel, the figure shows all decay curves with compositions found in Table I. For 20 mM CTAC observed at 0.8 ns/channel, the CPyrC concentrations are, from top to bottom, 0, 0.12, 0.16, 0.24, 0.33, 0.40, and 0.47 mM CPyrC. For 40 mM CTAC observed at the shorter time increment, the CPyrC concentrations are those given in Table I, but the decay in the absence of CPyrC is not shown. For the same surfactant concentration, observed at the longer time increment, the CPyrC concentrations are, from top to bottom, 0, 0.24, 0.48, 0.60, and 0.94 mM CPyrC.

the parameters k_0 and k_q were linked in the global mapping table, whereas F_0 and $\langle n \rangle$ were local parameters.

3.2. Interpretation of the Model Parameters To Obtain the Aggregation Numbers. By use of eq 4 the

Table II. Aggregation Numbers ($\langle a \rangle_m$ and $\langle a \rangle_w$) and Polydispersity Indices for the Various CTAC Solutions, Calculated by Means of Equations 5 and 6[a]

	7 mM CTAC		10 mM CTAC		20 mM CTAC		40 mM CTAC	
	I	II	I	II	I	II	I	temp, °C
$\langle a \rangle_m$					87.2		93.4	10
$\langle a \rangle_w$					89.0		94.1	
$\sigma/\langle a \rangle_w$					0.23		0.07	
$\langle a \rangle_m$	68.6	69.1	73.4	74.8	80.8	82.5	92.6	20
$\langle a \rangle_w$	94.7	103.8	93.1	99.6	88.4	99.7	96.2	
$\sigma/\langle a \rangle_w$	0.71	0.76	0.63	0.71	0.41	0.59	0.22	
$\langle a \rangle_m$					75.1		85.9	30
$\langle a \rangle_w$					84.2		82.5	
$\sigma/\langle a \rangle_w$					0.46		0.34	

[a] Identical samples were measured at time increments equal to ~0.8 ns/channel (I) and ~1.7 ns/channel (II) with anthracene (5.6 ns) and 1-cyanopyrene (21.6 ns) as references, respectively. For 20 and 40 mM CTAC the results from measurements at 10 and 30 °C are also given.

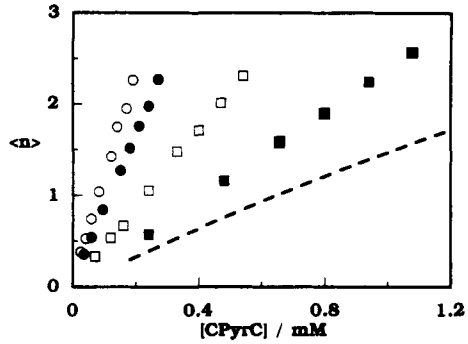

Figure 2. Average quencher occupancy number, $\langle n \rangle$, from computer fittings (see Table I) versus the quencher concentration; see eq 5. The symbols denote the following: open circles, 7 mM CTAC; filled circles, 10 mM CTAC; open squares, 20 mM CTAC; filled squares, 40 mM CTAC. The broken line is the result obtained by recalculation of data from ref 22 for a highly polydisperse system; see text.

aggregation numbers, $\langle a \rangle$, can be calculated. If one uncritically compares aggregation numbers at the same $\langle n \rangle$ value (e.g., $\langle n \rangle \approx 1$) for the different CTAC concentrations, one would draw the conclusion that higher surfactant concentrations definitely would lead to an increase in aggregation number. This is, however, not a satisfactory way to interpret data from fluorescence quenching measurements. Such an interpretation would be extremely "local" by nature, as it neglects the use of global interpretations, i.e., neglecting the relations between data obtained at different quencher concentrations. Furthermore, with a broad range of quencher concentrations in η space, see eq 6, one may, and should, check for polydispersity effects. We will in the two following subsections interpret the data with the assumption that the micellar aggregates are monodisperse and polydisperse, respectively.

3.2.1. Interpretation under the Assumption That the Aggregates Are Monodisperse. If one assumes monodisperse aggregates, allowing the use of eq 5, one can calculate the "monodisperse" aggregation number $\langle a \rangle_m$. As is seen in Figure 2, all surfactant concentrations yield straight lines through the origin with acceptable regression coefficients. From this it is tempting to conclude that the aggregates grow upon increasing surfactant concentration; the obtained aggregation numbers are summarized in Table II. Even if, for a monodisperse system, a straight line through the origin is a necessity when eq 5 is plotted, one must remember that this does not prove the monodispersity (or, better, a very narrow polydispersity) of the system. Inserted in Figure 2 (the broken line) are data for a simulated polydisperse micellar solution.[22] For this system, with an aggregation number (number average) of 60 and with $\sigma = 60$, it turns out that at low η values eq 5 still holds. Thus, the obtained results are not enough to judge the system to be monodisperse.

3.2.2. Interpretation under the Assumption That the Aggregates Are Polydisperse. The weight-averaged aggregation number, $\langle a \rangle_w$, can be calculated with use of eq 6. If the size distribution in the system is skewed, a plot of $\langle a \rangle_q$ versus η should not yield a straight line, whereas for a symmetrical distribution it should. From Figure 3, the resulting $\langle a \rangle_w$ are summarized in Table II; it can be concluded that there is a pronounced polydispersity with a skewed distribution at low surfactant concentrations. Increasing the surfactant concentration does not cause any substantial growth of the aggregates, as judged by $\langle a \rangle_w$, but causes the size distribution to be less polydisperse, as can be seen from the evaluation of the polydispersity index $\sigma/\langle a \rangle_w$ with surfactant concentration; see Table II.

One may argue that, if excluding the point at the lowest η value, one could fit a straight line to the remaining points. This would imply a much lower polydispersity as well as a symmetrical size distribution around the mean. From the model, however, a pronounced increase in $\langle a \rangle_q$ at low η is expected for a skewed distribution, as $\langle a \rangle_q \rightarrow \langle a \rangle_w$ when $\eta \rightarrow 0$. The pattern seen in Figure 3 has been observed earlier,[24d] justifying the inclusion of the $\langle a \rangle_q$ values at the lowest η values in the fits. Furthermore, for all CTAC concentrations, $\langle a \rangle_q$ takes about the same value at the lowest η value. This is as expected for a skewed polydisperse system, as, at low quencher concentrations, one will effectively only measure the quenching process in the larger aggregates. The uncertainty in quencher concentration, combined with a possible quencher distribution between the micelles and the aqueous bulk, makes the results from the lowest CTAC concentration the least reliable. At the highest CTAC concentration, however, these uncertainties are much smaller or absent, and, as the results at these two extremes can be satisfactory compared with each other, the conclusions drawn from the fittings shown in Figure 3 are valid. In the fittings of eq 6 to the data, only the points represented with the filled symbols in Figure 3 were used, due to the fact that the fitted polynomial function could show a minimum, whereas eq 6 must not show such a minimum.[23a]

Obviously the possible conclusion that could be made from the treatment described in the previous subsection, that the micelles grow upon addition of surfactant, is not the whole truth. When characterizing micellar systems, it is thus highly recommended to check for polydispersity effects. This requires measurements at many quencher concentrations, covering as large a region in η space as possible. Even if covering a large region, it is not certain that the use of eq 5 only will indicate polydispersity.

In Figure 4 the obtained aggregation numbers with use

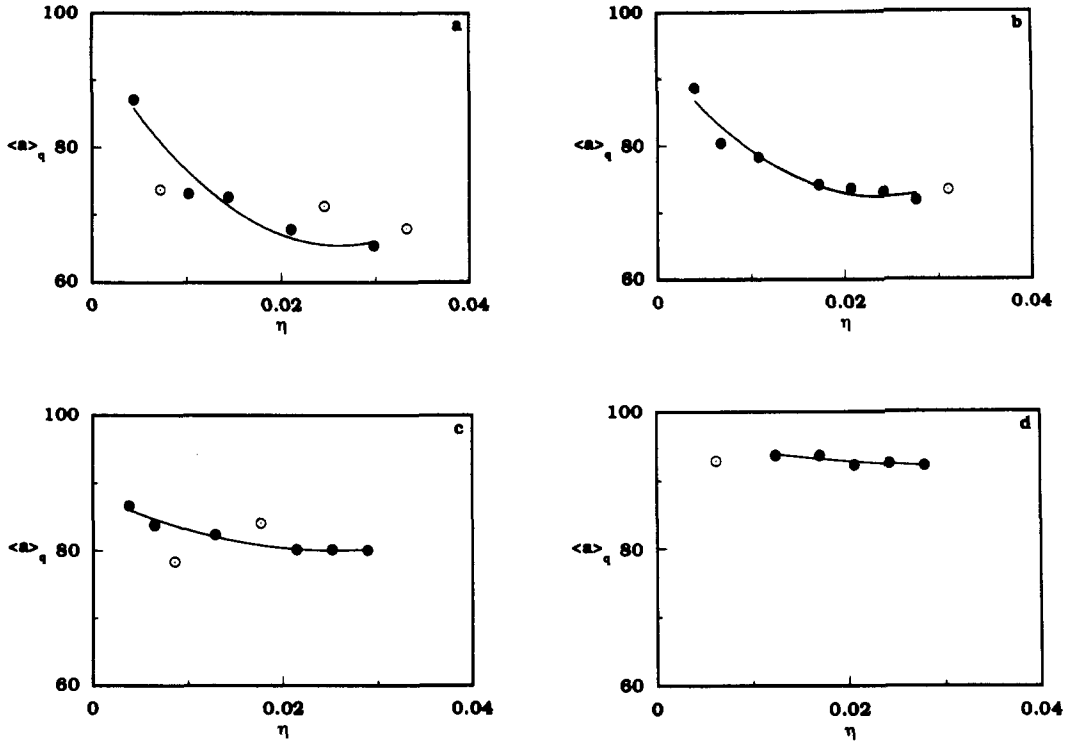

Figure 3. Quencher-averaged aggregation number, $\langle a \rangle_q$, versus the quencher-to-surfactant ratio, η, together with the fits obtained with use of eq 6. Filled symbols denote data used in polynomial fittings, eq 6. The four graphs show (a) 7 mM CTAC, (b) 10 mM CTAC, (c) 20 mM CTAC, and (d) 40 mM CTAC.

Table III. Occupancy Numbers ($\langle n \rangle$) for CPyrC and Aggregation Numbers ($\langle a \rangle_q$) for 20 and 40 mM CTAC at 10, 20, and 30 °C[a]

20 mM CTAC						40 mM CTAC					
10 °C		20 °C		30 °C		10 °C		20 °C		30 °C	
$\langle n \rangle$	$\langle a \rangle_q$	$\langle n \rangle$	$\langle a \rangle_q$	$\langle n \rangle$	$\langle a \rangle_q$	$\langle n \rangle$	$\langle a \rangle_q$	$\langle n \rangle$	$\langle a \rangle_q$	$\langle n \rangle$	$\langle a \rangle_q$
0.564	88	0.538	84	0.515	80	0.567	91	0.576	93	0.559	90
1.120	87	1.057	82	0.986	77	1.162	94	1.162	94	1.085	87
		1.484	84					1.598	94	1.484	87
1.863	87	1.715	80	1.598	75	1.917	93	1.909	92	1.781	86
		2.015	80			2.273	94	2.247	92	2.074	85
2.520	87	2.314	80	2.157	75	2.617	94	2.572	92	2.375	85
$k_q = 0.78$		$k_q = 1.23$		$k_q = 1.80$		$k_q = 0.81$		$k_q = 1.04$		$k_q = 1.58$	

[a] The time increment was ~0.8 ns/channel. The standard deviation on the aggregation numbers is estimated to be ±8%. The quenching rate constants, k_q, are given at the bottom of the table (10^7 s^{-1}).

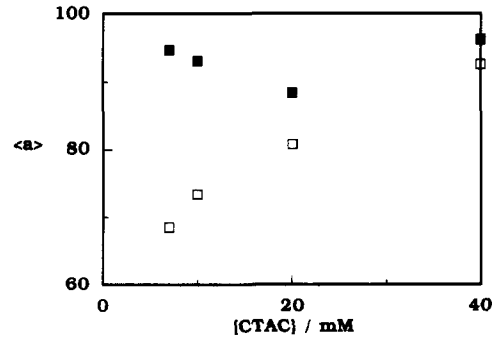

Figure 4. Aggregation number obtained from the measurements at the shorter time increment versus surfactant concentration: open symbols, the "monodisperse" aggregation number $\langle a \rangle_m$ obtained by use of eq 5; filled symbols, the weight-averaged aggregation number $\langle a \rangle_w$ obtained by use of eq 6.

of the two different interpretations are graphically shown, $\langle a \rangle_m$ from the assumption of monodisperse and $\langle a \rangle_w$ from polydisperse aggregates, clearly showing the difference in the results from the two interpretations.

3.3. Temperature Effects. To check for temperature effects, the samples with 20 and 40 mM CTAC were also measured at 10 and 30 °C. The fluorescence decay curves, Figure 5, all show well-developed, parallel tails at long times. The obtained aggregation numbers, $\langle a \rangle_w$, are graphically shown in Figure 6 and summarized in Table III. Increasing the temperature leads to small, but significant, changes in the micellar aggregation numbers. For thermodynamic and kinetic reasons[9b,30a] one would expect a decrease in aggregation number with increasing temperature, which is indeed found. The polydispersity, as judged by the polydispersity index, clearly increases with increasing temperature, Table II, and shows, thus, a temperature dependence, as is expected from thermodynamics.[46] Indeed, if the mean aggregation number does not increase on increasing temperature, one would, from thermodynamics, expect an increase in polydispersity.[46]

Increasing the temperature could increase the mobility of the probe and/or the quencher. It turned out from fittings of a generalized model of the Infelta–Tachiya model,[40,41] allowing both probe and quencher migration, that the temperature increase did not cause any detectable migration.

(46) Israelachvili, J. *Intermolecular & Surface Forces*, 2nd ed., Academic Press: New York, 1991; Chapter 16.

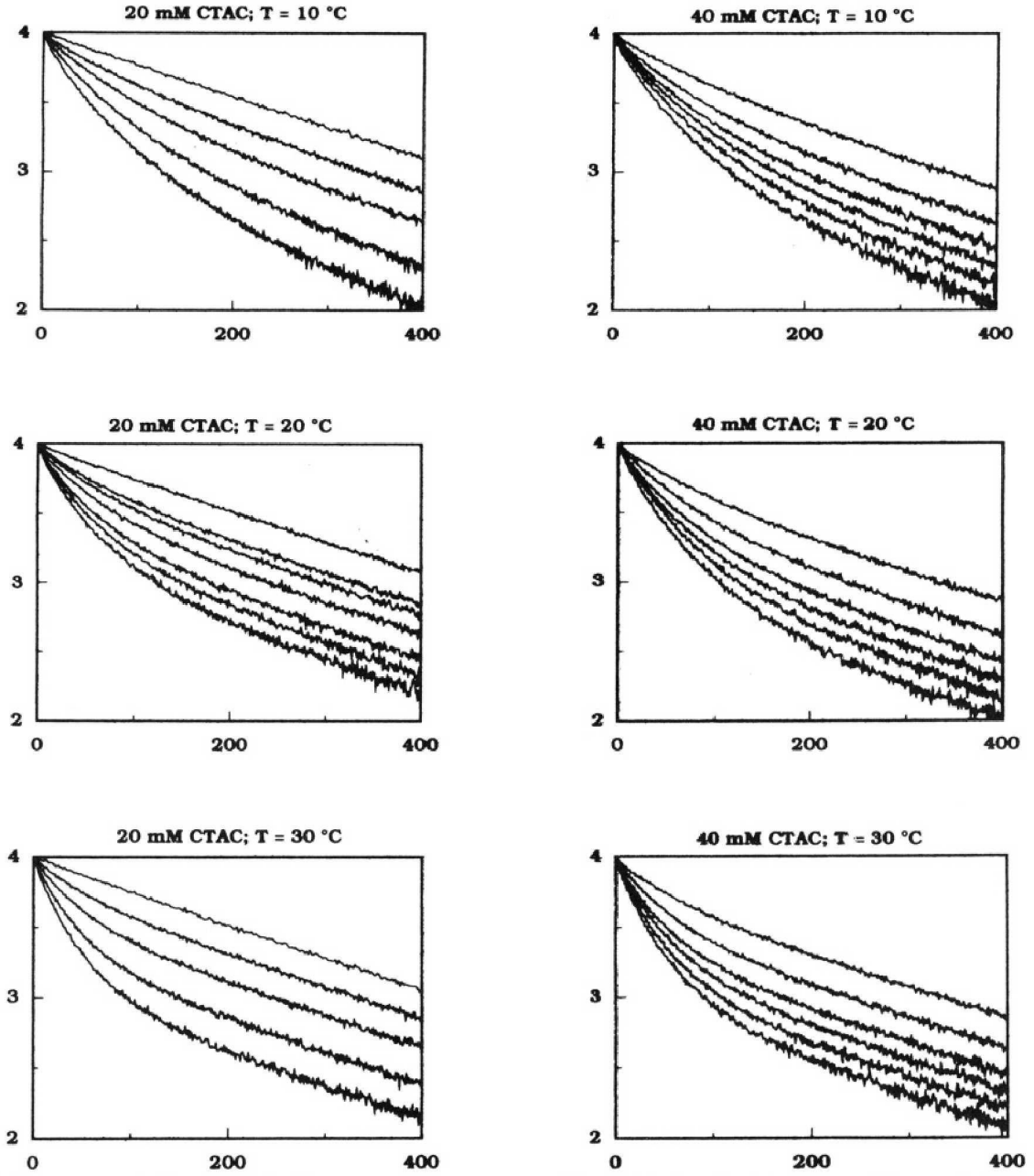

Figure 5. Temperature influence on the fluorescence decay pattern. The x axis gives the time (ns) and the y axis the logarithm of the (normalized) amount of counts per channel.

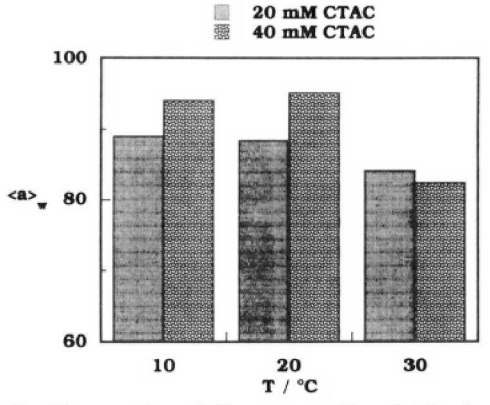

Figure 6. Temperature influence on the obtained weight-averaged aggregation number $\langle a \rangle_w$, as obtained by use of eq 6.

3.4. Quenching Rate Constant k_q. The parameter k_q has been linked in every set of fittings, although one may argue that, due to the polydispersity of the micellar aggregates and the assumed inverse proportionality between k_q and the micellar size (see, e.g., refs 5 and 7), the experimentally obtained k_q values should be a function of the quencher concentration and not constant. An increase of the surfactant concentration from 7 to 40 mM caused a decrease of the quenching rate by 25% (see Table I), which could be attributed to a growth of the micelles, since, for a diffusion-controlled process, the quenching rate constant should decrease with increasing micellar volume.

However, the statistical variation on the parameter $Z(\chi_\nu^2)$ and the fact that both the local and global values of this parameter in all cases are acceptable (see Table I) justify the linking of k_q.

One possible conclusion, taking both the aggregation behavior and the changes in k_q into account, is that there is in fact a micellar growth on increasing surfactant concentration, but that this growth preferably changes the size of the smaller aggregates formed close to the cmc. This would simultaneously lead to a decreased polydispersity as well as a slower observed average quenching

rate. This conclusion is supported by the fact that almost the same $\langle a \rangle_q$ is obtained at the lowest η value, as discussed above. If the larger aggregates do not grow upon increasing surfactant concentration, one should indeed obtain about the same $\langle a \rangle_q$ at low quencher concentrations.

A second result from the fittings, the regular, but small, increase in lifetime with increasing surfactant concentration (see Table I), also supports this idea. In a polydisperse micellar solution, the probe molecules solubilized in the smaller aggregates will experience a less hydrophobic environment due to deeper water penetration. The same effect has been reported in the case of surfactant–polymer systems.[16] As the smaller aggregates grow upon addition of more surfactant to the system, this effect will decrease.

3.5. Choice of Time Increment. In this paper two different time increments were used. In general terms, the total time window (the time increment multiplied by the number of channels) must be broad enough to allow the development of the quencher-concentration-independent part of the decay. It is known from other measurements[39] that when the quenching is slow or the probe or the quencher migrates, a too narrow time window can lead to wrong conclusions. In the present case, however, the quenching is fast enough and both probe and quencher are stationary, allowing the use of a narrower time window. The advantage of a shorter time increment is that the initial, nonexponential decay, showing the quenching kinetics, will be better described. On the other hand, a longer time increment will lead to a more pronounced exponential tail, and as it is possible to obtain the occupation number, $\langle n \rangle$, by extrapolating $e^{-k_0 t}$ back to time $t = 0$ for the tail (at long times eq 3 takes the form $F_t = F_0 e^{-k_0 t - \langle n \rangle}$), a broader time window would give more accurate estimates of the aggregation number. In our opinion, however, one should combine, if necessary, different time windows and evaluate the obtained data in a global manner with appropriate linking of parameters to obtain reliable estimates on k_0, $\langle n \rangle$, and k_q.

4. Conclusions

A dynamic fluorescence quenching study was performed at four different surfactant concentrations, each with eight different quencher concentrations, in the CTAC–1-MePy–CPyrC system. From global fittings of appropriate models to the experimental data, the weight-averaged aggregation numbers and polydispersity parameters were estimated. These estimations, together with the changes in the rate constant of quenching and the lifetime of the excited probe, let us conclude that the system exhibits a rather broad polydispersity in micellar aggregation numbers at low surfactant concentration. Increasing the surfactant concentration leads to a growth of the smaller micelles and, thus, to a more narrow size distribution. These findings may have important impact on the general view on micellar dynamics and stability.

The measurements performed with two different time increments lead to equivalent estimates of the parameters.

The micellar aggregation number decreases and the polydispersity increases, as expected, with increasing temperature.

Acknowledgment. S.R. is a research assistant of the NFWO. D.B. is indebted to Comisión de Investigaciones Científicas de la Provincia de Buenos Aires (CIC) and Katholieke Universiteit Leuven for a fellowship. M.G. is indebted to CNPQ (Brazil) and Katholieke Universiteit Leuven for a fellowship. J.v.S. is a visiting postdoctoral scientist at Katholieke Universiteit Leuven, sponsored by fellowships from Katholieke Universiteit Leuven and The Swedish Institute. M.V.d.A. is an "Onderzoeksleider" of the FKFO. The Belgian Ministry of Scientific Planning and Programmation is thanked for continuing support through Grants IUAP-III-040 and IUAP-II-16. N. Boens is thanked for the development of the global analysis software.